

A Scale Free Model of Ventilation-Induced Lung Injury

Drew C. Gottman^{1,2}, Bradford J. Smith²

¹ University of Colorado School of Medicine | Anschutz Medical Campus, Aurora, CO

² Department of Bioengineering, University of Colorado Denver | Anschutz Medical Campus, Aurora, CO

Rationale

- Mechanical ventilation is a necessary life-saving intervention for patients with acute respiratory distress syndrome (ARDS)
- Ventilation can also exacerbate ARDS and further propagate lung injury
- Previous studies have found that lung injury is heterogeneous; however, our understanding of injury heterogeneity is incomplete.**
- Improving on existing models of lung injury heterogeneity may facilitate development of more protective ventilation modalities**

Methods

- Mice were subjected to a two-hit injury model of pulmonary lavage and ventilator-induced lung injury
- Histological lung cross sections were prepared and whole slide images were recorded
- Areas of pulmonary edema and atelectasis – two markers of lung injury – were segmented with the machine learning software Ilastik
- We conceptualized the dynamics governing lung injury as analogous to earthquakes using network model that assigns correlations between injury regions based on size and distance apart**
- We found evidence of “injury hubs” and rich-get-richer behavior that govern injury progression**

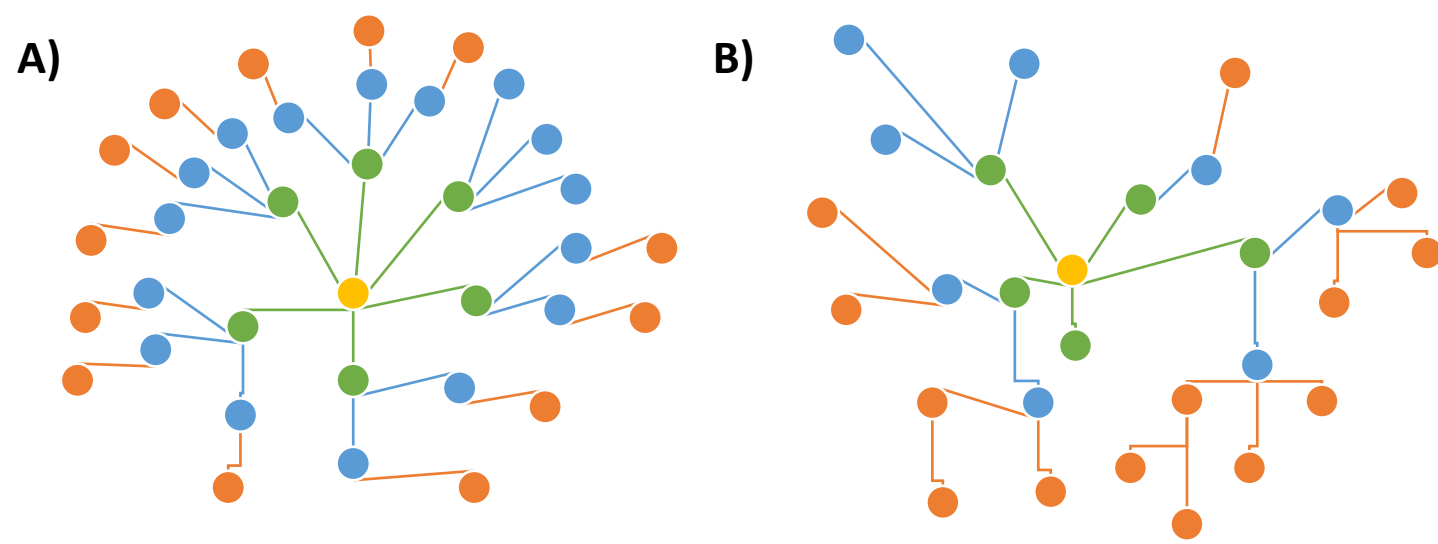


Figure 1. Representative graphs of a scale-free network (A) and a random network (B).

Segmentation Results

Human Scored Class	Ilastik Predicted Class		
	Injury	Air	Other
	Injury 333	6	87
Air	3	453	12
Other	144	21	381

Figure 2. Confusion matrix of human classification versus automated pixel classification using Ilastik for the three pixel classes: ‘Injury’, ‘Air’, and ‘Other’. Rows are human scores while columns are Ilastik scores. For each tissue section, twenty pixels from each class were manually scored.

- Ilastik demonstrated good sensitivity and specificity for pixel classification compared to human classification
- Injury pixels
 - Sensitivity: 78%
 - Specificity: 85%
- Air pixels
 - Sensitivity: 97%
 - Specificity: 97%
- Other pixels
 - Sensitivity: 69%
 - Specificity: 89%
- Overall accuracy: 81%

Results: Injury Clusters

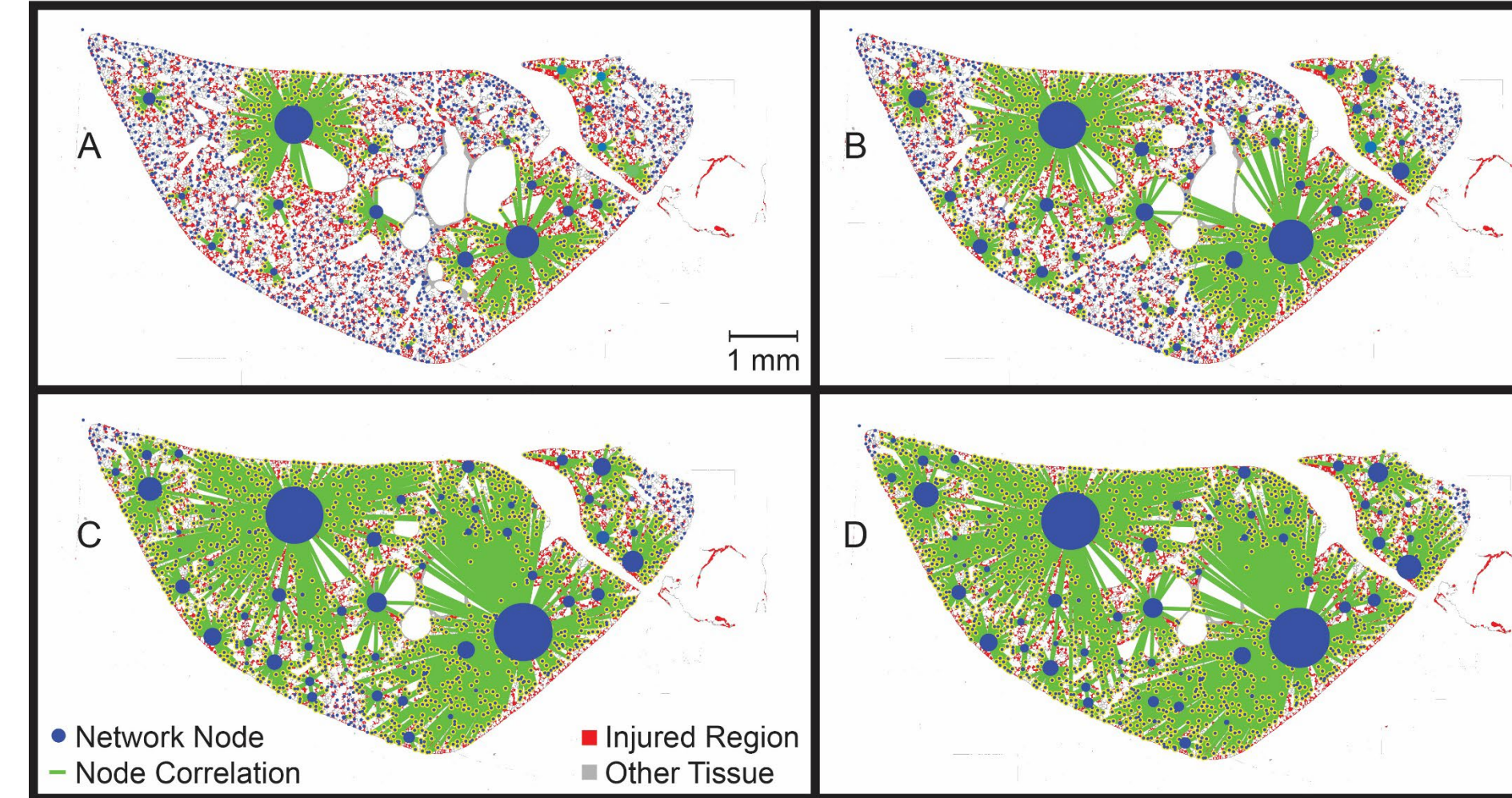


Figure 3. The strength of correlations between different injured areas are elucidated by varying the threshold n_c according to percentiles of $n_i \times n_j$. (A) has a threshold at the 25th percentile, (B) at the 50th percentile, (C) at the 75th percentile, and (D) at the 90th percentile. Injured pixels are red, while other tissue is grey. Nodes of the network, corresponding to discrete, injured regions, are denoted with a blue circle and green lines represent correlations between nodes in the network. The number of correlations that a given injured region receives is directly proportional to the size of the blue circle representing that injured region.

- Each injured region j is assigned a color according to the injured region i that j is connected to in the network
- Weaker correlations are eliminated according to the threshold assigned with smaller thresholds being more stringent
- This allows us to correlate and cluster regions of injury with varying levels of confidence and minimal visual clutter

Conclusions

- Regional correlations of earthquakes have similarities with those governing acute and ventilator-induced lung injury**
- Our model allows us to correlate regions of injury with minimal assumptions of the actual mechanism**
- Our model is generalizable to a variety of injuries, allowing for inspection of subtle patterns of injury heterogeneity**

Results: Secondary Injury Events

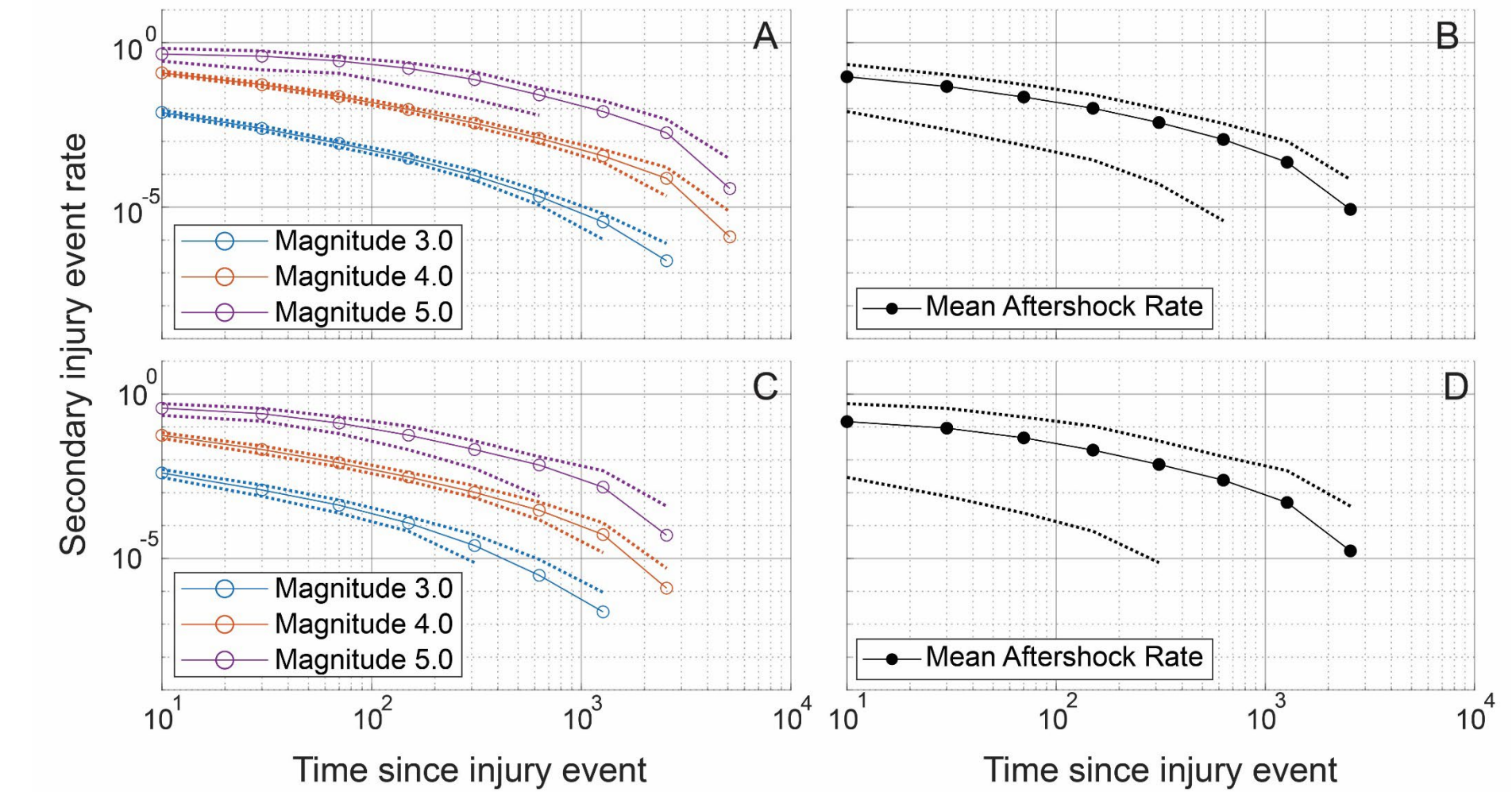


Figure 4. Simulated secondary injury event rates after a primary injury event are shown for randomly chosen CTRL (A, B) and LAV (C, D) sections. Simulated secondary injury event rates are shown separated by magnitude (A, C) and not separated by magnitude (B, D). 95% confidence bands are plotted for each magnitude and for the aggregated magnitudes. Injury magnitudes (sizes) are shown in a \log_{10} scale, analogous to the Richter scale, with a reference injury size of 1. Secondary injury event rates approximate power-law behavior with clear separation between secondary injury event rates at different magnitudes. Exponential binning is used to obtain approximately equal sample sizes in each time bin.

- Each injury event was randomly assigned a point in time and this process was repeated 100 times.
- Injuries were correlated using proximity across space and time as well as injury size.
- Injury event rates were plotted across time like aftershocks would be plotted after an earthquake.
- Pattern is similar to Omori’s law from seismology.

Acknowledgements & Financial Disclosures

- This research was made possible by Grants R00HL128944, from the National Institutes of Health. The contents are solely the responsibility of the authors and do not necessarily represent the official views of the NIH.
- I have no financial disclosures to report**